Defense Technical Information Center
Compilation Part Notice

ADP014395

TITLE: Mechanical and Microstructural Properties of Stratum Corneum

DISTRIBUTION: Approved for public release, distribution unlimited

This paper is part of the following report:

TITLE: Materials Research Society Symposium Proceedings. Volume 724. Biological and Biomimetic Materials - Properties to Function

To order the complete compilation report, use: ADA418623

The component part is provided here to allow users access to individually authored sections of proceedings, annals, symposia, etc. However, the component should be considered within the context of the overall compilation report and not as a stand-alone technical report.

The following component part numbers comprise the compilation report:
ADP014393 thru ADP014424

Mechanical and Microstructural Properties of Stratum Corneum

Kenneth S. Wu[1], William W. Van Osdol[2], and Reinhold H. Dauskardt[3]
[1]Department of Mechanical Engineering, Stanford University, Stanford, CA 94305-2205
[2]ALZA Corporation, Mountain View, CA 94039-7210
[3]Department of Materials Science and Engineering, Stanford University, Stanford, CA 94305-2205

ABSTRACT

A mechanics approach is presented to study the intercellular delamination resistance and mechanical behavior of stratum corneum (SC) tissue in the direction normal to the skin surface. The effects of temperature and hydration on debonding behavior were also explored. Such understanding, which includes the relationship of mechanical behavior to the underlying SC cellular structure, is essential for emerging transdermal drug delivery technologies. Fracture mechanics-based cantilever-beam specimens were used to determine reproducibly the energy release rates to quantify the cohesive strength of human SC. The debond resistance of fully hydrated SC was found to decrease with increasing temperature, while dehydrated SC exhibited a more complex variation with temperature. Stress-separation tests showed that fracture energies and peak separation stresses decreased with increasing temperature and hydration, although the SC modulus varied only marginally with temperature and hydration. Results are described in terms of microstructural changes associated with hydrophilic regions and intercellular lipid phase transitions.

INTRODUCTION

As the most externally exposed organ in the human body, the skin provides mechanical protection and a controlled permeable barrier to the external environment to maintain internal homeostasis. The layered construction of the skin represents a composite material in which the components possess specialized functionalities to accommodate a variety of conditions from mechanical stresses to variable ambient moisture and to resist the presence of toxic chemicals, pathogens, and radiation.[1] The top layer of the skin, the epidermis, consists of epithelial cells bound together via various cell-adhesion mechanisms including intercellular proteins and lipids. The top most layer of the epidermis, the stratum corneum (SC), consists of layered anucleated cells that mature and subsequently detach in a natural renewing process. The disk-shaped SC cells, composed largely of aligned keratin filaments, create a regular interdigitating structure held together by lipid and protein structures as illustrated in Fig. 1.

The SC is the first structure to provide resistance to abrasion and penetration of foreign objects and must provide this protection under highly variable temperature, humidity, and chemical conditions which bodily self-regulation or external environments may induce. In the case of emerging transdermal drug delivery technologies, the application and removal of adhesive drug delivery devices necessitates an appropriate balance between patch adhesive strength and SC cohesive strength in the direction normal to the skin surface. While previous investigators have examined in-plane properties of SC to determine modulus and fracture phenomena and dependencies upon environmental conditions, surprisingly little quantitative work has examined properties of the SC in the direction normal to the skin surface.[2,3,4,5,6,7] The resistance of SC to delamination is not well characterized, and virtually no quantitative data or reproducible test methods are available.

In the present study, a mechanics approach to examine the SC intercellular delamination resistance and out-of-plane mechanical behavior and their relationship to SC cellular structure is presented. The delamination resistance of human SC was examined as a function of selected testing and preconditioning temperature and moisture conditions and related to underlying structure. Fracture resistance was quantified in terms of the energy required to propagate a crack or debond and defined in terms of the strain energy release rate G, measured in units of J/m^2. Furthermore, stress-separation tests were performed to examine the out-of-plane mechanical behavior of the SC.

EXPERIMENTAL

Double-cantilever beam (DCB)

The debond resistance of human cadaver SC tissue was examined using fracture mechanics techniques developed to measure the adhesive properties of highly viscoelastic pressure sensitive adhesives.[8] Similar techniques have been employed to measure the adhesive properties of polymer bone cements.[9] The technique involves sandwiching the SC between two elastic polycarbonate substrates with cyanoacrylate adhesive to form fracture-mechanics based double-cantilever beam (DCB) specimens. The SC was separated from the underlying epidermis via a trypsin enzymatic digest then stored at 4°C in a fully hydrated state on water-moistened filter paper. The transparent polycarbonate beams facilitated optical inspection of the inner sandwich structure during sample preparation and testing. Substrate dimensions were chosen to ensure purely elastic deformation of the substrates during testing to enable the use of linear elastic fracture mechanics to determine the strain energy release rates.[8,9] Two sets of DCB specimens were prepared containing SC that was either fully hydrated (FH) or room-humidity dehydrated (DH) in 100% R.H. or 45% R.H. environments, respectively.

To fabricate the specimens, a thin layer of cyanoacrylate adhesive was applied to the face of a 40 mm x 10 mm x 3.175 mm polycarbonate substrate leaving a 7-10 mm region of the beam end uncoated. The substrate was pressed against the SC on the filter paper backing and a scalpel was used to cut around the substrate to detach the adhered SC from surrounding tissue. Another substrate coated with adhesive in the same manner was pressed against the SC face on the complimentary beam with adhesive-free ends aligned to form the final sandwich structure. Excess adhesive along the sandwich edges was removed with a scalpel to ensure that only SC was binding the two halves of the sandwich structure together.
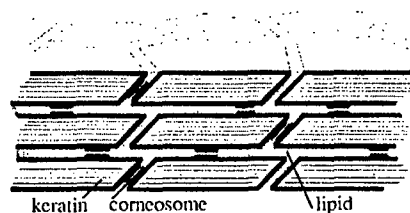

Figure 1. Schematic of the stratum corneum showing cellular structure including aligned keratin filaments as well as lipid intercellular space with corneosomes.
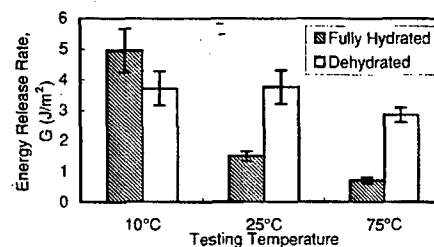

Figure 2. SC debond resistance values measured at selected temperatures after being fully hydrated or dehydrated. Error bars represent standard error of the mean.

Specimens were placed in an environmental chamber at selected temperature (10, 25, 75°C) and relative humidity (45 and 85% RH) conditions and allowed to equilibrate for ~10 min. Subsequently, the samples were loaded, via attached loading tabs, to propagate a debond within the SC layer. The specimens were tested in a custom-built mechanical test system with a computer controlled DC servoelectric actuator operated in displacement control. Tests were performed at a constant displacement rate of 2 μm/s. Corresponding loads were measured using a 222 N load cell and the debond length was determined using compliance techniques. Debond resistance was determined from critical values of the strain energy release rate, G_c.[8,9]

Stress-separation (SS)

Structures containing the SC sandwiched between polycarbonate substrates were fabricated in a similar manner to the DCB specimens. The substrate dimensions were 10 mm x 10 mm x 3.175 mm. The specimens were loaded normal to the SC face via attached loading tabs in an environmental chamber with controlled temperature and humidity. Testing was conducted at a constant displacement rate of 1 μm/s, yielding a strain rate of ~0.025 s^{-1} in the SC for a SC thickness of 40 μm. The SS measurements were performed using the same apparatus as that for DCB experiments. The specimens were allowed to equilibrate for ~20 min. before testing.

Scanning electron microscopy (SEM)

Both DCB and SS samples were examined after mechanical testing using SEM to characterize the debond surface morphologies. Selected specimens were allowed to dry in a desiccator and then gold coated and examined in an SEM operating at 15 keV. Two specimens from each testing condition were inspected to ensure representative characterization.

RESULTS

Debond resistance values, G_c, for specimens containing DH and FH SC measured at selected temperatures are presented in Fig. 2. All reported results are from testing utilizing a single sheet of SC to avoid tissue variations. The specimens exhibited constant debond energy with debond extension suggesting that the varying strain rates obtained during debond extension did not significantly effect the debond fracture resistance. Such behavior was subsequently verified by varying the testing displacement rate from 2 to 8 μm/s with no systematic effect on G_c values. The hydrated state of the SC had only a small effect on G_c values measured at 10°C where the average G_c value for the FH specimen was ~1 J/m^2 (or 25%) higher than the DH specimen. At elevated temperatures, the FH specimens exhibited markedly lower debond energy with increasing test temperature. In contrast, the DH samples lacked a pronounced change with temperature although a marginal decrease was apparent at 75°C. At the elevated temperatures, G_c values for the DH specimens were markedly higher than those of the FH specimens.

Stress-separation tests performed on DH and FH specimens under the same environmental conditions as the DCB tests are shown in Fig. 3(a). The SS tests resulted in linear loading up to a peak stress after which the stress catastrophically dropped essentially to zero. Any residual stresses decayed to zero with continued displacement. For the FH specimens tested at 75°C, the SS curves do not show the marked drop in stress but rather decrease more gradually from the peak stresses toward zero. The area enclosed by the SS curve represents the total work required to cause failure of the SC and resulting fracture energy values calculated from the SS curves are presented in Fig. 3(b). Similar to the DCB results, the SS fracture energy values of the FH specimens decreased markedly with increasing temperature while the DH specimens
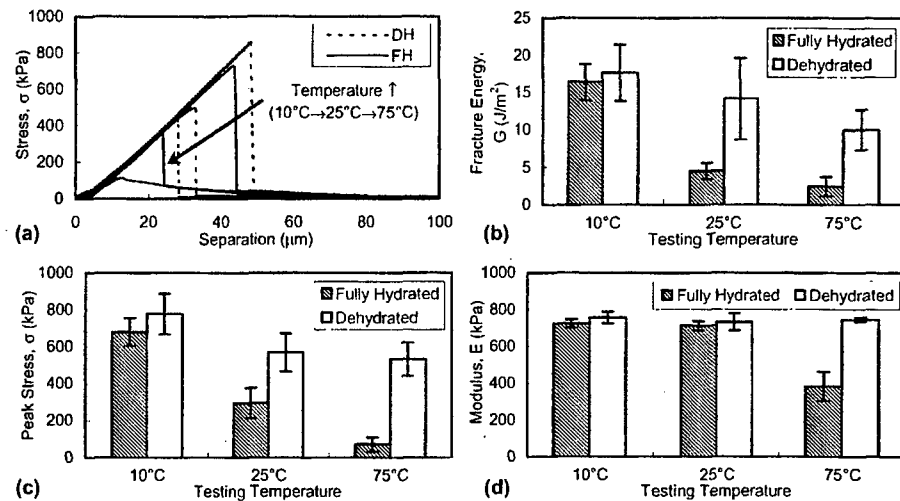
Figure 3. Stress-separation measurements conducted at selected temperatures showing (a) representative stress-separation curves, (b) fracture energy values determined from the area enclosed by the curves, (c) peak stresses, and (d) the initial loading modulus.

decreased less dramatically. Peak stress values obtained from the SS curves are shown in Fig. 3(c). Similar to the facture energy values, both the peak stresses and corresponding strains were observed to decrease with increasing hydration and testing temperature.

The initial stiffnesses (or moduli) of the SC in the out-of-plane orientation for the selected testing conditions are shown in Fig. 3(d). The SC modulus measured was ~0.7 MPa and was constant over the range of temperatures and hydrations tested with the exception of the FH specimens at 75°C where the modulus was ~ 0.4 MPa.

Representative SEM micrographs of the fracture surfaces of tested DCB specimens containing FH and DH SC are shown in Fig. 4. Similar micrographs were obtained for all testing types and conditions. The FH specimens revealed comparatively little surface morphology and individual SC cells were difficult to discern (Fig. 4(a)). The DH specimens all revealed partial pullout of individual SC cells to varying degrees producing more debond surface roughness. The SS tests reveal similar trends to those seen in the DCB specimens in which the DH specimens exhibit SC cell pullout while the FH specimens lack similar cellular features.

DISCUSSION

The marked decrease in fracture energy (Fig. 2) apparent with increasing temperature for the FH SC tissue are most likely related to a corresponding decrease in the peak cohesive strength (Fig. 3(c)) measured using the SS tests. Other energy dissipation mechanisms such as plasticity in the SC are also expected to scale with the peak cohesive strength. However, it should be noted that plastic deformation will be restricted in these specimens due to the thin film nature of the samples and the plane strain constraint of the DCB test configuration. The similarly constrained SS test geometries also limit plasticity. With restricted plastic zone formation, the SS data primarily represent properties of the cohesive mechanisms operating in

the SC layers. The limited influence of plasticity-type effects is seen by the similar trends in both DCB and SS fracture energy measurements and plastic zone calculations of ~0.1-0.5 μm. In the case of strong plasticity, one might expect to observe increasing G-values with hydration and temperature for the DCB tests. Therefore, the decreases in peak stresses and total work to failure with increasing temperature in SS tests correlate with lowered SC cohesive strength.

In comparison to the FH specimens, the DH SC exhibited far smaller changes in fracture energy and peak cohesive strength with increasing temperature, suggesting that the cohesive strength is strongly hydration dependent and more weakly associated with testing temperature. One possible explanation is related to the microstructure of the SC layer itself. In a simplistic model of the SC structure proposed by Elias et al.[10], the cells are viewed as highly keratinized bricks surrounded by a lipid mortar as represented in Fig. 1. In this model, behavior of the SC is presumed to be dominated by the properties of the lipids, particularly since the composition of the extracellular components are estimated to be at least 80 wt.% lipid.

Examination of the SEM micrographs reveals little overall difference in the extent of cellular pullout for the DH SC tissue tested at different temperatures suggesting that this feature of the debonding process is temperature independent. The FH specimen surfaces consistently remained quite featureless throughout the range of testing temperatures despite a large decrease in G_c values with increasing temperatures. Clearly, cellular pullout during debonding is therefore dependent on the initial hydration of the SC tissue. However, the lack of any significant morphological changes on the fracture surfaces of the FH specimens despite a correspondingly strong decrease in debond energy suggests that temperature must affect underlying processes that control the peak cohesive strength.

To better understand the possible effects of underlying SC structure upon the observed mechanical behavior, selected studies are briefly reviewed. X-ray diffraction (XRD) analysis of human SC revealed a crystalline structure associated with the lipids sheathing the keratin filaments that lie in the plane of the SC layer.[11] These results together with in-plane dynamical mechanical analysis (DMA) revealed hydration independent transitions that are attributed to lipid conformational changes from a crystalline to more disordered state.[2] Additionally, differential scanning calorimetry (DSC) analyses suggest that the presence of strong endothermic dips in the gathered data indicate transitions in the SC due to variations in water content; the in-plane modulus was also observed to decrease with increased testing humidity.[3] From the DSC analysis these changes were attributed to keratin fiber relaxation due to substitution of existing protein-protein hydrogen bonds with water-mediated bonding facilitating greater fiber mobility, as these bond substitutions would lead to a reduction in modulus with increasing hydration level.
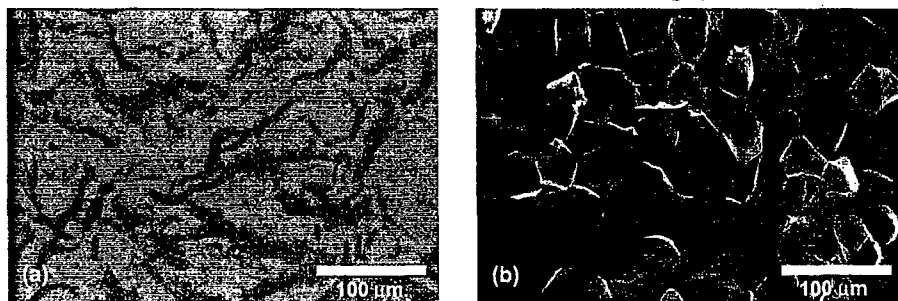

Figure 4. Scanning electron micrographs of DCB specimens. Fully hydrated (a) and Dehydrated (b) samples tested at 25°C.

While the mechanisms responsible for the out-of-plane properties are different, some insight can be gathered from the analyses reported above. As suggested by Papir et al.[3], the ability of water molecules to substitute for existing hydrogen bonds may lead to strength degradation. Thus, while the lipid transitions may be hydration independent as indicated by XRD tests, mechanical degradation may require the presence of water to facilitate loss of structural integrity and cohesive strength; so, the proportionally smaller decreases in fracture energies and peak stresses in the DH samples may be explained by the lack of hydration available to mediate weakening mechanisms. Additionally, the decreases in fracture energy with increasing temperature may be a result of greater accessibility of hygroscopic sites to water molecules leading to bond substitution as the lipid structure becomes more disorganized.

Furthermore, in contrast to in-plane modulus data, the moduli measured during SS testing reveal a behavior that is quite distinct from the changes observed during in-plane testing.[3,4] The modulus values shown in Fig. 3 indicate little variation with hydration or temperature although the cohesive strengths of the samples decrease as seen in the reported total work to failure. While the abrupt decrease in out-of-plane modulus (Fig. 3(d)) may seem anomalous, the measured value can be explained upon closer examination of the SS curves. The SC exhibits an increase in stiffness for separations less than ~10 μm, but due to substantially decreased cohesive strength, the FH SC tested at 75°C begins to fail before stiffening occurs.

Comparing in-plane with out-of-plane mechanical properties reveals that the simplistic model proposed by Elias et al.[10] requires refinement to explain the results presented here. For example, the in-plane tensile tests performed by Papir et al.[3] on newborn rat SC led to measurements of decreasing elastic moduli ranging from ~8.87 GPa to 12 MPa with increasing humidity at constant temperature while similar tests by Wildnauer et al.[4] upon human SC revealed moduli decreasing from ~45 MPa to 10 MPa, assuming a SC thickness of 40 μm. Similar decreases in modulus with increasing temperature were observed as well.[3] These values are starkly different from the out-of-plane measurements of ~0.7 MPa. Furthermore, only limited work to measure in-plane fracture properties of human SC as a function of varying environmental conditions has been performed. Koutroupi and Barbenel[5] have measured mean fracture energies of 3600 J/m^2 for ~76% RH conditioned SC samples in a tearing configuration, and subsequent work by Nicolopoulos et al.[6] suggests that debond energy increases with increasing hydration, a trend not generally observed in the DCB or SS specimens. Intuitively, the in-plane fracture energy is expected to be higher than that of the natural delamination mode. However, that the fracture energy is orders of magnitude greater than the ~1-6 J/m^2 measured in delamination tests is surprising.

In the bricks-and-mortar model, the mechanical characteristics of the SC should be the same in both orientations provided the mortar is isotropic. However, the data discussed above indicate that the SC exhibits much tougher in-plane mechanical characteristics as compared to those out-of-plane. While mechanical anisotropy is evident, the mechanisms causing the differences are unclear but may be related to additional SC microstructure. In transmission electron microscope (TEM) studies, remnants of desmosomal structures, or corneosomes, are evident between SC cells.[12] Structurally important in the lower levels of the epidermis, these structures are located where intermediate filaments such as keratin fibers terminate in one cell wall and bridge the intercellular space to connect to adjacent cells. Although the corneosomes are thought to be degraded desmosomes, these structures may facilitate the transmission of tensile forces between cells leading to the greater stiffnesses and higher fracture energies observed in this orientation. Furthermore, considering the alignment of the keratin fibers in the

plane of the SC layer, increased mobility of the fibers with increasing hydration as postulated by Papir et al.[3] represents a reasonable mechanism leading to decreased modulus with increased fiber sliding. Further exploration remains necessary to determine the precise microstructural mechanisms that lead to the observed mechanical properties; however, the bricks and mortar model needs refinement (Fig. 1) in order to capture the true mechanical properties of the SC.

CONCLUSION

A fracture-mechanics based approach using DCB specimens was developed to examine quantitatively the delamination properties of stratum corneum. In conjunction with out-of-plane stress-separation measurements, a decrease in debond energy with increasing temperature was observed in fully hydrated SC tissue. Little effect of testing temperature was observed for dehydrated SC tissue. The observed decrease in debond energy was associated with a reduction in SC cohesive strength due to hydration-mediated processes. While fracture energy decreases with increasing hydration for tests above 25°C, it remains unclear why G-values are higher for the fully hydrated samples at 10°C. Measurements of modulus obtained while varying temperature and hydration reveal that SC stiffness in this mode is much lower than that reported in-plane. The fracture energy and modulus data reveal that a simple bricks and mortal model requires refinement to explain the highly anisotropic mechanical behavior exhibited by the SC.

ACKNOWLEDGMENTS

REFERENCES

1. A.J. Thody and P.S. Friedmann in *Scientific Basis of Dermatology: A Physiological Approach*, edited by A.J. Thody and P.S. Friedmann (Churchill Livingstone, Inc., London, 1986), p. 1-5.
2. G.L. Wilkes and R.H. Wildnauer, *Biochimica et Biophysica Acta* **304**, 276 (1973).
3. Y.S. Papir, K.-H. Hsu, and R.H. Wildnauer, *Biochimica et Biophysica Acta* **399**, 170 (1975).
4. R.H. Wildnauer, J.W. Bothwell, and A.B. Douglass, *The Journal of Investigative Dermatology* **56**, 72 (1971).
5. K.S. Koutroupi and J.C. Barbenel, *Journal of Biomechanics* **23**, 281 (1990).
6. C.S. Nicolopoulos, P.V. Giannoudis, K.D. Glaros, and J.C. Barbenel, *Archives of Dermatological Research* **290**, 638 (1998).
7. M.A. Wolfram, N.F. Wolejsza, and K. Laden, *The Journal of Investigative Dermatology* **59**, 421 (1973).
8. M. B. Taub and R. H. Dauskardt in *Biomaterials for Drug Delivery and Tissue Engineering*, edited by S. Mallapragada, R. Korsmeyer, E. Mathiowitz, B. Narasimhan, and M. Tracy, (Mater. Res. Soc. Proc. **662**, Warrendale, PA, 2001) pp. NN4.9.1-NN4.9.6.
9. K.L. Ohashi, A.C. Romero, P.D. McGowan, W.J. Maloney, and R.H. Dauskardt, *J. Ortho. Res.*, **16**, 705 (1998).
10. P.M. Elias, S. Grayson, M.A. Lampe, M.L. Williams, and B.E. Brown in *Stratum Corneum*, edited by R. Marks and G. Plewig (Springer-Verlag, Berlin, 1983), p. 53-67.
11. G.L. Wilkes, A.-L. Nguyen, and R. Wildnauer, *Biochimica et Biophysica Acta* **304**, 267 (1973).
12. J. Vičanová, A.M. Mommaas, A.A. Mulder, H.K. Koerten, and M. Ponec, *Cell Tissue Research* **286**, 115 (1996).